Effects of shape and composition on the properties of CdS nanocrystals

Soumendu Datta, Mukul Kabir, and Tanusri Saha-Dasgupta
Department of Condensed Matter Physics and Material Sciences, S.N. Bose National Centre for Basic Sciences, JD Block, Sector-III, Salt Lake City, Kolkata 700 098, India

(Received 16 February 2012; revised manuscript received 22 August 2012; published 5 September 2012)

Using first-principles electronic structure calculations, we studied the relative stability between hexagonal wurtzite (WZ) and cubic zinc-blende (ZB) structures and the electronic properties of the CdS nanocrystals of varying shape and surface composition. Our study shows substantial enhancement of the stability of the WZ phase over that of the ZB phase upon moving from a spherical to a cylindrical shape. Our study provides microscopic understanding of the dominant stability of the WZ phase in cylindrically shaped nanocrystals. The calculated band gaps also show interesting variation as a function of varying shape and surface composition.

DOI: 10.1103/PhysRevB.86.115307 PACS number(s): 73.22.−f, 71.15.Mb, 78.67.−n, 78.55.Et

I. INTRODUCTION

Semiconductor nanocrystals with dimensions smaller than the bulk excitonic Bohr radius constitute a class of materials intermediate between bulk semiconductors and those of molecules.[1,2] Quantum confinement of excitons leads to an increase in the band gap with decreasing crystal size. Such a variation has been exploited recently in various applications such as solar cells,[3,4] optoelectronics,[5] catalysis,[6] as well as in clinical diagnoses.[7]

The II-VI semiconductor CdS has a large bulk excitonic Bohr radius (∼3 nm),[8] and its size evolution due to the quantum confinement effect is dramatic.[1] The band gaps of CdS vary between 4.8 and 2.5 eV as the size is varied from a nanocluster of 1.3 nm to macroscopic crystals.[9] The lifetime of the lowest allowed optical excitation ranges from tens of a picosecond to several nanoseconds.[1] Furthermore, for CdS, which is well known for polytypism between hexagonal wutzite (WZ) and cubic zinc-blende (ZB) symmetry based structures in bulk phases,[10] the reduction in particle size seems to influence the structural stability.[11] Previously, we have shown[11] that the Cd-rich quantum dots (QDOTs) in the strong confinement regime (<2.5 nm) stabilize in the WZ phase, while the S-rich QDOTs stabilize in the ZB phase. Our study revealed that a change of covalency is the responsible factor for such a composition dependent stability. Since the band gaps are known to exhibit[11,12] a dependence on the underlying symmetry of the nanocrystal, knowledge of the symmetry of a nanocrystal with a given size and shape is crucial. While most studies are focused on QDOTs with a spherical shape, many fewer studies have been carried out for quantum rods (QRODs). The reported studies[13–23] are also mostly focused on the influence of shape change on band gap rather than on crystallographic structures, apart from a few exceptions. For example, one experimental study[19] reports on the stability of the WZ phase for QRODs as opposed to the expected cubic ZB phase in QDOTs. The computational study,[24] carried out on another semiconductor nanocrystal, InP, revealed the role of dangling bonds (DBs) on the facets of QRODs in the stabilization of the WZ phase. Such a study is needed for CdS, for which the issue of polytypism is even more serious than InP due to smaller energy differences between the WZ and ZB phases in bulk.[10,24] Also it is not entirely clear whether the DB at the surface is the sole player in the structural stability since the CdS nanocrystals synthesized experimentally are passivated, thereby diminishing the DB effects.

In this paper, we have performed a comprehensive analysis to study the interplay between size, shape, and composition for the CdS nanocrystals. We considered the effect of passivation simulating through pseudohydrogen in order to disentangle the DB effect from other possible effects that may dominate the stability. We find that the change of shape has a dramatic effect on the structural stability. Upon increasing the aspect ratio, the stability of the WZ phase is found to be greatly increased over the ZB phase. This is found to flip the stability behavior from ZB to WZ in moving from a spherical shape to a cylindrical shape in cases of stoichiometric as well as Cd- or S-rich nanocrystals upon an increase of the aspect ratio $\geqslant$1.6. We find an enhanced stability of the WZ phase in the cylindrical geometry in the presence of passivation as well as allowing for full relaxation of the atoms. This hints at the fact that factors beyond surface morphology are operative in the stabilization of the WZ phase in QROD geometry. Our study shows that the change in the strength of covalency in QROD geometry compared to that in QDOT geometry to be the key factor driving the enhanced stability of the WZ phase in QROD geometry, which gets helped by the DB effect in the case of bare nanocrystals.

Focusing on the band gap, we find that in general the band gap increases (blueshifted) upon moving from QDOTs to QRODs, in agreement with some experimental observations.[19] Interestingly, the effect of surface chemistry brings in nontrivial effects.

II. CONSTRUCTION OF QRODs

The structural transformation from the WZ to ZB phase involves a change in symmetry from hexagonal to cubic, while keeping the nearest neighbor atomic coordination fixed at four. Here we have employed a specific way to build the QROD/QDOT structures to enable studying the relative stability of different crystal phases. This also helps us to construct structures with various possible surface chemistries, which will be the realistic situation in experiments. For the construction of QRODs, we choose the experimental growth direction [111] for the ZB phase and [0001] for the WZ phase,[19,25] instead of cutting out from a structure of a bulk supercell, in which case it

TABLE I. Compositional and geometric details of stoichiometric CdS nanocrystals for WZ and ZB structures. For comparison we have also considered infinite ZB and WZ QRODs. The lengths and diameters of the finite nanocrystals are given in Å. n, n_{Cd}, n_{S}, n^{surf}, and n_{db} represent the total number of atoms, number of Cd and S atoms, number of surface atoms, and number of dangling bonds, respectively, in the constructed nanocrystals.

	$n(n_{\mathrm{Cd}}+n_{\mathrm{S}})$		n^{surf}		n_{db}		Aspect ratio (length/diameter)	
Systems	ZB	WZ	ZB	WZ	ZB	WZ	ZB	WZ
I	206 (103 + 103)	210 (105 + 105)	102	104	240	206	3.4 (42.18/12.33)	3.0 (37.55/12.36)
II	156 (78 + 78)	172 (86 + 86)	78	86	186	176	2.6 (32.45/12.33)	2.5 (30.87/12.36)
III	196 (98 + 98)	176 (88 + 88)	90	80	168	156	1.7 (27.68/16.44)	1.4 (22.54/16.49)
IV	184 (92 + 92)	192 (96 + 96)	74	78	182	198	1.0 (22.65/22.65)	1.0 (21.44/21.44)
Infinite QROD	184 (92 + 92)	186 (93 + 93)	86	72	138	126	∞	∞

is difficult to control the surface morphology and composition. To generate "cylindrical" QRODs, we first considered the consecutive atoms along the growth directions, and then the nanocrystal structures were obtained by adding the nearest neighbor translation vectors of the respective symmetry with the atomic positions along the axis.

We studied the relative stability between the ZB and WZ phases as a function of the aspect ratio of QRODs for three different classes of systems: (1) stoichiometric QRODs, (2) nonstoichiometric Cd-rich QRODs, and (3) nonstoichiometric S-rich QRODs. For each of these three cases, we have considered four systems (I–IV) with varied aspect ratios (the aspect ratio decreases along I→IV), where system IV represents a spherical QDOT with an aspect ratio of 1. Additionally, for stoichiometric QRODs, we have considered the case of an infinite rod with bulklike periodicity along the growth direction. An attempt has been made to keep the total number of atoms, aspect ratio, and the degree of nonstoichiometry (in the case of nonstoichiometric QRODs) as similar as possible between the ZB and WZ phases for each system, to make them energetically comparable.

For stoichiometric QRODs, we have first considered an even number of Cd and S atoms along the growth direction, and the bond center of the central two atoms was taken as the center of the rod. The chemical composition, shape, and surface geometry for stoichiometric QRODs thus constructed are detailed in Table I. The number of DBs (listed in Table I) are calculated as $n_{\mathrm{db}} = \sum_{i=1}^{n^{\mathrm{surf}}}(4 - z_i)$, where n^{surf} is the total number of surface atoms, and z_i is the coordination of the ith surface atom in the nanocrystal. The aspect ratio is calculated as the ratio of length along the growth direction and the diameter along the lateral direction. We note that while the QRODs studied in Ref. 24 had a hexagonal or triangular cross-sectional shape with well-defined facets, that is not the case in the present study.

For nonstoichiometric QRODs, we considered an odd number of Cd and S atoms along the growth direction, with the central atom as the center of the rod. Thus, CdS QRODs become either Cd or S rich depending on the choice of the central atom (Cd or S) along the growth direction. Similar to the stoichiometric case, we have considered ZB and WZ structures for both the Cd- and S-rich QRODs. The structural details are given in Table II for the S-rich QRODs. Such details for the Cd-rich systems can be obtained by interchanging the identity of the Cd and S atoms.

III. COMPUTATIONAL DETAILS

We have conducted density functional calculations for the constructed nanocrystals. We used the projector augmented wave pseudopotential,[26,27] and the Perdew-Burke-Ernzerhof exchange-correlation functional[28] as implemented in the Vienna *ab initio* simulation package.[29] The total electronic energies were evaluated at a kinetic energy cutoff of 280 eV, which gives sufficient convergence of total energy to compare the relative stability of various phases. To check the validity of our applied methodology, we computed the cohesive energies of bulk WZ and ZB phases. In agreement with previous results,[10] we found that bulk CdS stabilizes in the WZ phase with a cohesive energy of −2.65 eV/atom. The ZB structure is found to lie only 9.7 meV/atom higher in energy, also in agreement with a previous result.[10]

The nanocrystals are placed in a periodic cubic supercell such that the images were separated by at least 12 Å. We have considered in selected cases the relaxation of the surface atoms as well as relaxation of all the atoms in nanocrystals in

TABLE II. Compositional and geometric details of S-rich nanocrystals for ZB and WZ phases. Unlike the stoichiometric nanocrystals, the number of Cd and S atoms are different for all the systems, which are shown in the parentheses. The degree of nonstoichiometry, defined as $\mathcal{D}_{\mathrm{ns}} = (1 - \mathrm{Cd/S})$ in the case of S-rich systems for both ZB and WZ structures, increases with decreasing aspect ratio.

	$n(n_{\mathrm{Cd}}+n_{\mathrm{S}})$		$n^{\mathrm{surf}} = n^{\mathrm{surf}}_{\mathrm{Cd}} + n^{\mathrm{surf}}_{\mathrm{S}}$		n_{db}		$\mathcal{D}_{\mathrm{ns}}$		Aspect ratio (length/diameter)	
Systems	ZB	WZ	ZB	WZ	ZB	WZ	ZB	WZ	ZB	WZ
I	191 (88 + 103)	194 (89 + 105)	96 (36 + 60)	97 (36 + 61)	222	184	0.15	0.15	3.4 (42.18/12.33)	3.0 (37.55/12.36)
II	141 (63 + 78)	156 (70 + 86)	72 (24 + 48)	79 (27 + 52)	168	154	0.19	0.19	2.6 (32.45/12.33)	2.5 (30.87/12.36)
III	169 (71 + 98)	210 (91 + 119)	78 (18 + 60)	92 (24 + 68)	162	196	0.28	0.24	1.7 (27.68/16.44)	1.4 (22.54/16.49)
IV	147 (55 + 92)	153 (57 + 96)	64 (0 + 64)	67 (0 + 67)	148	156	0.40	0.40	1.0 (22.65/22.65)	1.0 (21.44/21.44)

order to study the possible effect of relaxation on the structural stability. The positions of the atoms were relaxed towards equilibrium until the Hellmann-Feynman forces become less than 0.01 eV/Å.

In order to disentangle the effect of DBs from that of the electronic effect induced by the change of geometry, we saturated the DBs via passivation to remove the localized surface states that appear in the midgap region. Instead of large organic molecules that are used in experiments,[1] we used pseudohydrogens with a different nuclear charge to saturate the DBs. The atoms in both the ZB and WZ CdS phases are fourfold coordinated, and thus we used pseudohydrogen with a positive nuclear charge $z = (8 - m)/4$ to passivate the surface atom with m formal valence charge, as followed in the earlier work.[30] Therefore, to keep the system locally charged neutral, we used $H^{3/2}$ and $H^{1/2}$ to terminate the dangling bonds associated with the surface Cd and S atoms, respectively. Further, we used the optimized Cd-$H^{3/2}$ (1.82 Å) and S-$H^{1/2}$ (1.46 Å) bond lengths determined from two tetrahedrally coordinated model systems, $CdH_4^{3/2}$ and $SH_4^{1/2}$, respectively.

IV. RESULTS AND DISCUSSIONS

A. Structural stability: Unpassivated nanocrystals

Though in experiments the nanocrystals are passivated by some ligand, it has been theoretically shown that the relaxed structures are qualitatively the same for unpassivated and ligand-passivated cases.[31–33] Thus, we first analyze the relative stability between the ZB and WZ structures of the unpassivated nanocrystals with varying aspect ratio. This will also allow us to compare the structural stability of unpassivated and passivated nanocrystals, and disentangle the effect of dangling bonds, which is considered to be a dominant effect in structural stability. We calculated the cohesive energy per atom of the unpassivated nanocrystals as

$$E_c = \frac{1}{(n_{\mathrm{Cd}} + n_{\mathrm{S}})}[E^{\mathrm{tot}} - n_{\mathrm{Cd}}E_{\mathrm{Cd}} - n_{\mathrm{S}}E_{\mathrm{S}}], \qquad (1)$$

where E^{tot} is the total energy of the unpassivated nanocrystal, E_X is the energy of an isolated X atom, and n_X is the number of X atoms ($X = \mathrm{Cd/S}$). According to this definition, the cohesive energy is a negative quantity. Thus, more negative cohesive energy means higher stability. Our calculated cohesive energies for the stoichiometric as well as nonstoichiometric Cd- and S-rich unpassivated nanocrystals of both the ZB and WZ phases are shown in Fig. 1 with varied aspect ratio. First note that the infinite QROD stabilizes in the WZ phase, similar to the bulk CdS. For the systems with a finite aspect ratio, the cohesive energies show a substantially high stability of the WZ phase compared to the ZB phase for nanocrystals with a large aspect ratio. We find a structural transition from the ZB to WZ phase due to the change in nanocrystal shape from QDOT to QROD in the case of the stoichiometric and the S-rich systems. It is also interesting to note that upon increasing aspect ratio, the relatively small energy difference between WZ and ZB phases becomes larger (from few tens of meV to few hundreds of meV). This finding follows the trend reported in the experimental study[19] that indicates a preference for the WZ structure for long QRODs.

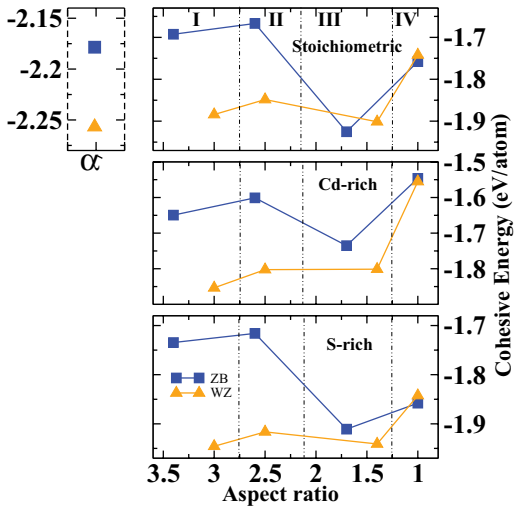

FIG. 1. (Color online) Calculated cohesive energies for the unpassivated (bare) stoichiometric (top panel), Cd-rich nonstoichiometric (middle panel), and S-rich nonstoichiometric (bottom panel) nanocrystals as a function of varying aspect ratio. The isolated data points shown in the top panel are for the infinite rod.

To understand the trend observed in the structural stability with varied aspect ratio in Fig. 1, we have calculated the surface energy contribution and variation of surface DBs for each system. The surface energy (per surface atom) is defined as $E_{\mathrm{SE}} = \frac{E^{\mathrm{clus}} - n\epsilon^{\mathrm{bulk}}}{n^{\mathrm{surf}}}$, E^{clus} being the total cohesive energy of the nanocrystal, and n and n^{surf} being the total number of atoms and surface atoms, respectively. ϵ^{bulk} is the bulk cohesive energy per atom. Note that the surface energy is a positive quantity according to the definition, and the higher surface energy corresponds to lower stability for the corresponding structure. Figure 2 shows the plot of calculated surface energy for each system in both the ZB and WZ structures. It is seen that the QRODs with a larger aspect ratio (systems I and II in Tables I and II) have lower surface energies in the WZ phase compared to the ZB phase. Thus, these structures for all the classes of systems, including the infinite QROD, stabilize in the WZ phase. In contrast, as the aspect ratio decreases (systems III and IV), the surface energy for stoichiometric and S-rich systems is lower in the ZB phase, which makes this phase more stable over the WZ phase. Note that for stoichiometric systems, such a variation in surface energy with the aspect ratio can be understood purely from the variation of the surface geometry of the nanocrystals. In this case, we find a direct correspondence between the average number of dangling bonds per surface atom and surface energy (cf. inset of the top panel of the Fig. 2, which shows the difference in dangling bonds between the ZB and WZ phases), and thus is inversely related with the stability.

In contrast to the stoichiometric systems, where we see that the stability of different crystal phases is dictated purely by the surface geometry effect, the relative stability in nonstoichiometric nanocrystals depends on both the surface geometry and the surface composition. Comparing the case of nonstoichiometric QDOTs and QRODs, we find an interesting interplay between the effects of surface geometry and surface chemistry. For nonstoichiometric QDOTs, the surface is monocomponent (completely of either Cd or S composition)

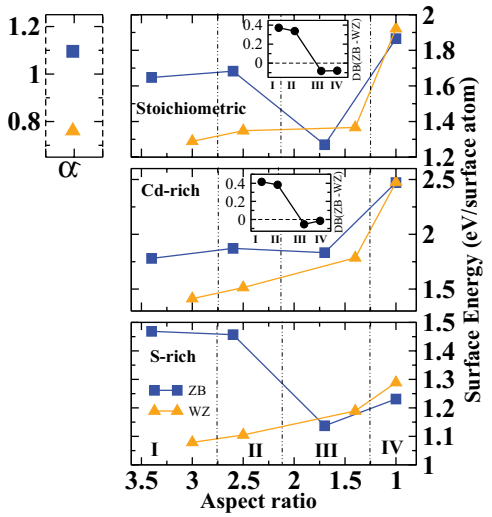

FIG. 2. (Color online) Calculated surface energies for the unpassivated (bare) stoichiometric (top panel), Cd-rich nonstoichiometric (middle panel), and S-rich nonstoichiometric (bottom panel) nanocrystals as a function of varying aspect ratio. The isolated data points shown in the top panel are for the infinite rod. The difference in dangling bonds between the ZB and WZ structures are shown in the insets of top panel (for the stoichiometric systems, I–IV) and middle panel (for nonstoichiometric systems, I–IV).

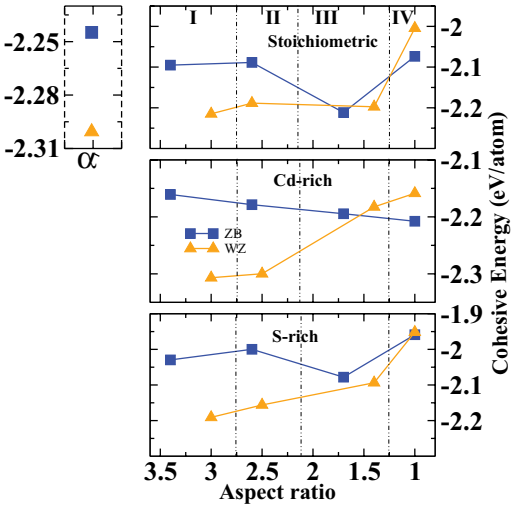

FIG. 3. (Color online) Cohesive energies for ZB and WZ structures plotted as a function of varying aspect ratio for stoichiometric (top panel) as well as Cd-rich (middle panel) and S-rich (bottom panel) H-passivated CdS nanocrystals.

while for nonstoichiometric QRODs it is of mixed composition with a major dominance of S (S-rich case) or Cd (Cd-rich case) and a minor presence of Cd or S, respectively. The structural stability of nonstoichiometric QDOTs is, therefore, determined predominantly by the surface chemistry effect, which takes over the weaker surface geometry effect. This is in the sense that while the analysis of DBs (in the inset of the middle panel of the Fig. 2) which capture the surface geometry effect predicts that the ZB phase should be more stable, in reality, depending on whether the surface is Cd or S covered, the ZB or WZ phase is stabilized.[11,34] For QRODs, on the other hand, the structural stability is determined by the strong surface geometry effect (as the difference of dangling bonds in the inset of the middle panel of Fig. 2 is $+ve$ for them) with the surface chemistry effect becoming less important. Irrespective of the dominance of Cd or S in the surface, the QRODs are found to be stable in the WZ phase with an increased stability beyond an aspect ratio of 1.6.

B. Structural stability: Passivated nanocrystals

Finally, an interesting question is what happens to the above structural stability analysis if one passivates the dangling bonds. This is also an important question since in the experimental synthesis condition the nanocrystals are passivated and the effect of dangling bonds, which formed a central point in the above described analysis, will be minimized. Cohesive energy per atom of the H-passivated CdS nanocrystals can be defined as

$$E_c = \frac{1}{(n_{\mathrm{Cd}} + n_{\mathrm{S}})}\big[E^{\mathrm{tot}} - n_{\mathrm{Cd}}E_{\mathrm{Cd}} - n_{\mathrm{S}}E_{\mathrm{S}} - n_{\mathrm{H}}E_{\mathrm{H}} - n_{\mathrm{H}}^{\mathrm{Cd}}E^{b}_{\mathrm{Cd\text{-}H}} - n_{\mathrm{H}}^{\mathrm{S}}E^{b}_{\mathrm{S\text{-}H}}\big], \quad (2)$$

where E_{tot} is the total energy of the passivated nanocrystal, E_X is the energy of an isolated X atom, and $E^b_{X\text{-H}}$ is the bonding energy of the isolated X-H dimer. n_X is the number of X atoms, and $n_{\mathrm{H}} = n_{\mathrm{H}}^{\mathrm{Cd}} + n_{\mathrm{H}}^{\mathrm{S}}$ is the total number of passivated H. Figure 3 shows the plot of the cohesive energy defined, as above, for the ZB and WZ structures as a function of varying aspect ratio, for both passivated stoichiometric as well as passivated nonstoichiometric nanocrystals. We find while the details change between the unpassivated and passivated system, especially for aspect ratios in the crossover region between the spherical to cylindrical geometry, the general trend of high stability of the WZ phase in QROD geometry holds well, even in the presence of passivation. This shows that the dominant stability of the WZ phase over the ZB phase for QRODs with a large aspect ratio has a common origin for unpassivated and passivated nanoclusters.

In order to check the influence of the structural relaxation, we have carried out full relaxation of the nanocrystal, considering the case of the passivated S-rich system II. Although a substantial relaxation has been observed for both the WZ and ZB phases, the trend in relative stability remains the same as in unrelaxed nanocrystals, in the sense that the WZ phase turned out to have a minimum energy structure. However, the energy difference between the phases decreases to 0.02 eV/atom, compared to ~0.15 eV/atom in the unrelaxed case. The atoms on the surface relax differently from the atoms in the bulk region of the nanocrystals, which is in qualitative agreement with previous studies on the $Cd_{33}Se_{33}$ nanocluster.[31–33] For the optimized WZ phase, the Cd-S bonds at the center of the QRODs are about 3% longer compared to the experimental bulk value. The atoms on the surface relax differently and the corresponding Cd-S bonds on the surface are 1.5% smaller compared to the same in the core region. This inhomogeneous relaxation indicates surface reconstruction. This also leads to a decrease in both Cd-Cd and S-S separation on the surface. Similar to the previously observed trend for passivated and bare CdSe nanoclusters,[31,32] we find that the distance between

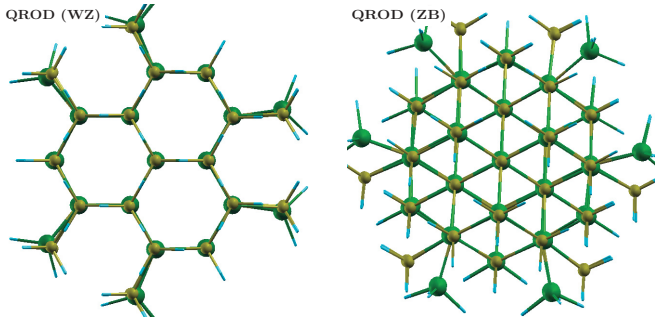

FIG. 4. (Color online) Structurally relaxed cross-sectional view of the passivated S-rich nanocrystals (system II) in both WZ and ZB phases. Large, green (medium, yellow) balls represent Cd (S) atoms, and the small, cyan colored balls represent H atoms.

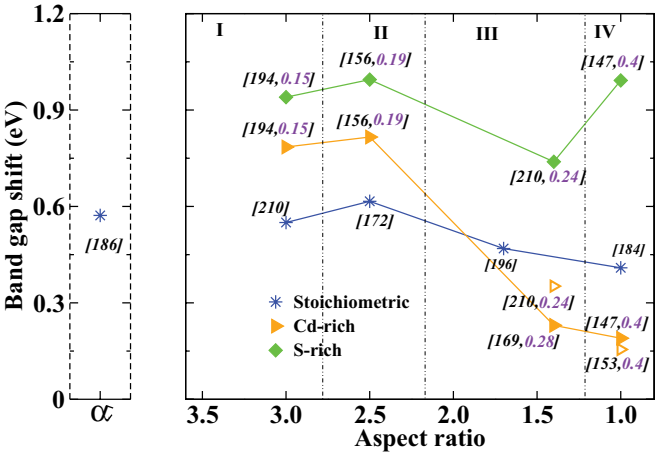

FIG. 5. (Color online) Shift in the band gap as a function of varying aspect ratios for the minimum energy phases of the stoichiometric, Cd-rich, and S-rich nanocrystals. The isolated data point for the stoichiometric infinite rod is shown in the left panel. The total number of atoms and the degree of nonstoichiometry (only in case of nonstoichiometric systems) are also marked for each data point. For Cd-rich system III and IV nanocrystals, the symmetry of the minimum energy structure changes between passivated and unpassivated cases. The data points corresponding to the minimum energy structure of the unpassivated cases are also shown as open symbols.

the two closest Cd atoms on the surface is shorter (∼4 Å) compared to ∼4.4 Å in the center of the QROD in the WZ phase. Similarly, for the S atoms on the surface the separation is ∼4.05 Å, compared to ∼4.5 Å between the nearest S in the center of the QROD. The relaxation for the ZB nanocrystal is quantitatively similar to the WZ phase as described. The cross-sectional views of the relaxed structures in the WZ and ZB phases are shown in Fig. 4.

In order to investigate the microscopic mechanism of this stabilization of the WZ phase in QROD geometry, we calculated the average charge enclosed within a sphere around a Cd atom and that around a S atom for both QROD (system I) and QDOT geometries and considering both ZB and WZ symmetries. Independent of the chosen symmetries, our calculation shows ≈0.1–0.15 more average electronic charge enclosed within the spheres around Cd and S atoms for QROD geometry compared to QDOT geometry, for which the average electronic charge shows more preference to occupy the bond connecting Cd and S atoms. This, in turn, indicates ionicity to be stronger in QROD, or in other words, the covalency to be weaker for QROD, compared to QDOT.

Tetrahedrally coordinated binary semiconductors of type $A^N B^{8-N}$ are known to exhibit ZB-WZ polymorphism, which is subtle due to the small energy differences involved and have been discussed in literature both in terms of model as well as first-principles calculations.[10,35] The general understanding that emerged out of all these calculations is that it is the competition between the covalency and the ionicity effects that determines the relative stability of ZB versus WZ structures in bulk. Covalency effects which favor isotropic distribution in turn favor the ZB structure while the ionicity favors the WZ structure. The calculation of the ionicity factor using a Wannier function based analysis[10] also brought out the same trend within the CdX series (X = S, Se, Te); CdS, being most ionic, stabilizes in WZ symmetry while CdSe and CdTe, being more covalent, stabilize in ZB symmetry.

In our previous study,[11] we discovered the same covalency effect to be operative to drive the ZB symmetry for S-terminated CdS nanoclusters and WZ symmetry for Cd-terminated CdS nanoclusters. The present study reveals that the enhanced stability of the WZ phase in QROD geometry is also governed by the change (weakening) of the Cd-S covalency due to the change in geometry. The DB effect in the case of bare nanocrystals, as described in the previous section, adds to this effect.

C. Band gaps

The calculated band gap [the highest occupied molecular orbital–lowest unoccupied molecular orbital (HOMO-LUMO) gap)] of the passivated systems in the minimum energy structures are shown in Fig. 5. We find the surface passivation moves the occupied surface states below the Fermi level, and the empty surface states are pushed higher in energy above the Fermi level, opening up the clean band gap in the passivated systems, and validating the scheme of passivation. As these band gaps are underestimated in conventional density functional theory (DFT) (1.59 eV for the bulk WZ and 1.52 eV for the bulk ZB CdS) compared to the experimental value of 2.42 eV, we are interested in their variation and not in the absolute values. In Fig. 5, we therefore plot the shift in band gap measured from the DFT band gap for the bulk CdS system. The band gap shifts are calculated for both stoichiometric as well as for nonstoichiometric nanocrystals. The band gap calculations have been carried out for the minimum energy structures in each case. This means WZ structures are considered for systems I and II. For system III, it is of ZB symmetry for stoichiometric and Cd-rich nanocrystals, and of WZ symmetry for S-rich nanocrystals. For system IV, it is of ZB symmetry.

We find that band gaps are in general larger for QRODs compared to QDOTs, with the exception of S-rich nanocrystals. We note that in our constructed CdS nanocrystals, though we made an effort to have a similar number of atoms between the different systems, they are not exactly same, which adds to the variation of band gap between systems on top of the primary effect of changing aspect ratio. Focusing on

stoichiometric and Cd-rich nonstoichiometric nanocrystals, we find in moving from system IV (QDOT with aspect ratio of 1) to the system III (with aspect ratio ∼1.6), the band gap increases, which increases further in moving to system II with an even higher aspect ratio, ∼2.5. Between systems I and II, the band gaps hardly change as the systems are already in the limit of long QRODs (with comparable width) and they behave similarly. For S-rich nonstoichiometric nanocrystals, this general trend is followed with an exception in the behavior of moving from system IV (QDOT) to system III. Instead of an increase, we observe a decrease. This is driven by the further effect of the variation in the degree of nonstoichiometry between systems IV and III. The degree of nonstoichiometry is high in QDOTs for which the surface is either entirely S or Cd covered, while for QRODs the degree of nonstoichiometry is smaller (∼0.2), having mixed characters of surface composition with a dominance of either S or Cd. In our earlier work for QDOTs,[11] we have shown that the band gaps associated with S-terminated clusters are much higher than that of Cd-terminated clusters (cf. Fig. 14 in Ref. 11). The dominance of S in the surface, therefore, gives rise to an increase in the band gap and the dominance of Cd in the surface gives rise to a decrease in the band gap. In moving from system IV to III, which amounts to moving from the QDOT to QROD regime, the degree of nonstoichiometry drops down significantly. This effect of variation in degree of nonstoichiometry in the case of S-rich systems acts in the opposite direction to the trend set by aspect ratio variation, while it acts hand in hand with the trend set by aspect ratio variation for the Cd-rich systems. It is, therefore, the surface chemistry effect that gives rise to these two opposite behaviors in the nature of band gap variation. Concerning the experimental situation, the compilation of experimental data on the band gap of CdS nanoclusters shows a much larger variation in band gaps compared to that of ZnSe and CdTe,[12] for which the polymorphism between WZ and ZB is less effective. It has been shown recently that CdS nanocrystals can be thermodynamically stabilized in both WZ and ZB crystallographic phases at will, just by the proper choice of the capping ligand,[36] which leads to S- and Cd-rich crystals. The rather large scatter in experimental data[12] may therefore be explained in terms of the variation in band gap between S- and Cd-rich clusters, though it has not been established certainly. More and careful experimental investigation is needed in this direction.

V. CONCLUSION

Using the first-principles electronic structure calculations, we have studied the effect of shape and composition on the structural and electronic properties of CdS nanocrystals. We found that, regardless of the composition, nonstoichiometric or stoichiometric CdS QRODs stabilize in the WZ phase, in agreement with the findings in Ref. 19. This is in contrast with QDOTs, where composition plays a major role in determining the phase stability. The relative stability of the WZ phase for QRODs is found to increase with increasing aspect ratio. Our findings turn out to be true both for bare as well as passivated nanocrystals. The microscopic origin of this general trend of the enhanced stability of the WZ phase in nanocrystals with a higher aspect ratio stems from the weakening of Cd-S covalency in moving from QDOT to QROD geometry. The choice of specific ligands, such as carboxyl ligands usually used for growth of CdS, may add further to this stabilization as the bonding to the carboxyl ligands may be favored in WZ geometry for QRODs. In general, the calculated band gap is found to increase in QRODs compared to QDOT. However, the surface composition may play a role, causing deviation from this general trend.

ACKNOWLEDGMENT

The authors thank the Department of Science and Technology, India for support through the Advanced Materials Research Unit and Unit for Nanoscience and Technology.

[1] A. P. Alivisatos, Science **271**, 933 (1996).
[2] M. Bawendi, M. Steigerwald, and L. Brus, Annu. Rev. Phys. Chem. **41**, 477 (1990).
[3] W. Huynh, X. G. Peng, and A. P. Alivisatos, Adv. Mater. **11**, 923 (1999).
[4] W. U. Huynh, J. J. Dittmer, and A. P. Alivisatos, Science **295**, 2425 (2002).
[5] V. I. Klimov, A. A. Mikhailovsky, S. Xu, A. Malko, J. A. Hollingsworth, C. A. Leatherdale, H. J. Eisler, and M. G. Bawendi, Science **290**, 314 (2000).
[6] T. S. Ahmadi, Z. L. Wang, T. C. Green, A. Henglein, and M. A. Elsayed, Science **272**, 1924 (1996).
[7] X. Huang, P. K. Jain, I. H. El-Sayed, and M. A. El-Sayed, Nanomedicine **2**, 681 (2007).
[8] L. E. Brus, J. Chem. Phys. **80**, 4403 (1984); Y. Wang and N. Herron, J. Phys. Chem. **95**, 525 (1991).
[9] T. Vossmeyer, L. Katsikas, M. Giersig, I. G. Popovic, K. Diesner, A. Chemseddine, A. Eychmüller, and H. Weller, J. Phys. Chem. **98**, 7665 (1994).
[10] C.-Yu Yeh, Z. W. Lu, S. Froyen, and A. Zunger, Phys. Rev. B **46**, 10086 (1992); **45**, 12130 (1992); S. Datta, T. Saha-Dasgupta, and D. D. Sarma, J. Phys.: Condens. Matter **20**, 445217 (2008).
[11] S. Datta, M. Kabir, T. Saha-Dasgupta, and D. D. Sarma, J. Phys. Chem. C **112**, 8206 (2008).
[12] S. Sapra and D. D. Sarma, Phys. Rev. B **69**, 125304 (2004); R. Viswanatha and D. D. Sarma, Chemistry–Asian J. **4**, 904 (2009).
[13] D. S. Xu, Y. J. Xu, D. P. Chem, L. G. Guo, L. L. Gui, and Y. Q. Tang, Adv. Mater. **12**, 520 (2000).
[14] D. Routketvitch, T. Bigioni, M. Moskovits, and J. M. Xu, J. Phys. Chem. **100**, 14037 (1996).
[15] F. Gao, Q. Y. Lu, S. H. Xie, and D. Y. Zhao, Adv. Mater. **14**, 1537 (2002).
[16] Y. W. Jun, S. M. Lee, N. J. Kang, and J. W. Cheon, J. Am. Chem. Soc. **123**, 5150 (2001).
[17] X. F. Duan and C. M. Lieber, Adv. Mater. **12**, 298 (2000).
[18] Y. W. Wang, G. W. Meng, L. D. Zhang, C. H. Liang, and J. Zhang, Chem. Mater. **14**, 1773 (2002).

[19]B. A. Simmons, S. Li, V. T. John, G. L. McPherson, A. Bose, W. Zhou, and J. He, Nano Lett. **2**, 263 (2002).
[20]H. Yu, J. Li, R. A. Loomis, L.-W. Wang, and W. E. Bhuro, Nat. Mater. **2**, 517 (2003).
[21]Y. Chen, J. Li, X. Yang, Z. Zhou, and C. Q. Sun, J. Phys. Chem. C **115**, 23338 (2011).
[22]M. Korkusinski, O. Voznyy, and P. Hawrylak, Phys. Rev. B **82**, 245304 (2010).
[23]S. Schulz and G. Czycholl, Phys. Rev. B **72**, 165317 (2005).
[24]T. Akiyama, K. Nakamura, and T. Ito, Phys. Rev. B **73**, 235308 (2006).
[25]J. Li and L.-W. Wang, Chem. Mater. **16**, 4012 (2004).
[26]P. E. Blöchl, Phys. Rev. B **50**, 17953 (1994).
[27]G. Kresse and J. Furthmuller, Phys. Rev. B **54**, 11169 (1996).
[28]J. P. Perdew, K. Burke, and M. Ernzerhof, Phys. Rev. Lett. **77**, 3865 (1996).
[29]G. Kresse and J. Hafner, Phys. Rev. B **47**, 558 (1993); **48**, 13115 (1993); **49**, 14251 (1994).
[30]L. W. Wang and J. Li, Phys. Rev. B **69**, 153302 (2004).
[31]H. Kamisaka, S. V. Kilina, K. Yamashita, and O. V. Prezhdo, J. Phys. Chem. C **112**, 7800 (2008).
[32]S. Kilina, S. Ivanov, and S. Tretiak, J. Am. Chem. Soc. **131**, 7717 (2009).
[33]A. Puzder, A. J. Williamson, F. Gygi, and G. Galli, Phys. Rev. Lett. **92**, 217401 (2004).
[34]S. Datta, M. Kabir, T. Saha-Dasgupta, and D. D. Sarma, J. Nanosci. Nanotechnol. **9**, 5489 (2009).
[35]G. A. Jeffrey, G. S. Parry, and R. L. Mozzi, J. Chem. Phys. **25**, 1024 (1956); F. Keffer and A. M. Portis, *ibid*. **27**, 675 (1957); J. C. Phillips and J. A. Van Vechten, Phys. Rev. Lett. **22**, 705 (1969); A. Zunger and M. L. Cohen, *ibid*. **41**, 53 (1978); N. E. Christensen, S. Satpathy, and Z. Pawlowska, Phys. Rev. B **36**, 1032 (1987).
[36]A. Nag, A. Hazarika, K. V. Shanavas, S. M. Sharma, I. Dasgupta, and D. D. Sarma, J. Phys. Chem. Lett. **2**, 706 (2011).